HYDROLOGICAL PROCESSES
Hydrol. Process. **18**, 3583–3594 (2004)
Published online in Wiley InterScience (www.interscience.wiley.com). DOI: 10.1002/hyp.5793

A deterministic method to characterize canopy radiative transfer properties

Timothy E. Link,[1]* Danny Marks[2] and Janet P. Hardy[3]

[1] *University of Idaho, Department of Forest Resources, PO Box 441133, Moscow, ID 83844-1133, USA*
[2] *USDA Agricultural Research Service, Northwest Watershed Research Center, 800 Park Blvd, Suite 105, Boise, ID 83712-7716, USA*
[3] *Engineering Research Development Center, Cold Regions Research and Engineering Laboratory, 72 Lyme Road, Hanover, NH 03755-1290, USA*

Abstract:

Investigations of snowcover dynamics beneath vegetation canopies require either measured or estimated solar and thermal radiation values at the snow surface. A deterministic method is presented that uses portable arrays of pyranometers and pyrgeometers to quantify the amount of incoming radiation at the snow surface. Example solar and thermal radiation datasets are presented from boreal deciduous, boreal coniferous and temperate coniferous forest stands. The data indicate that the canopies transmitted 33% (4–8 March), 15% (6–10 February), and 3% (22–24 September) of the above-canopy radiation. In the boreal deciduous and temperate conifer stands, thermal radiation is increased by 25% and 34% respectively. Thermal gains partially offset solar reduction, such that incoming all-wave radiation is decreased by 22% and 25% respectively for each of these stands. When recorded at a high temporal resolution, array data can estimate below-canopy diffuse solar radiation values for estimation techniques that treat direct and diffuse transmission independently. We provide examples of how radiometer array data are used to derive simple canopy radiation transmissivity parameters for global, beam and diffuse radiation. Radiometer arrays also provide data for detailed investigations to assess within-stand radiation variability, or to investigate radiation variations across land cover discontinuities, to advance our understanding of snowcover energetics in complex environments. Copyright © 2004 John Wiley & Sons, Ltd.

KEY WORDS snow hydrology; solar radiation; thermal radiation; forest canopy; radiative transfer; aspen; jack pine; Douglas fir

INTRODUCTION

Vegetation canopies affect snowcover energetics by shading the snow surface from solar radiation (0·28–3·5 μm), and by enhancing the incoming thermal radiation (3·5–100 μm). The accurate characterization of the radiative regime beneath forest canopies is essential for investigations focusing on snowcover, soil moisture, and ecological dynamics. Simulation of snowcover and soil energetics beneath forest canopies requires that solar and thermal fluxes are either measured beneath forest canopies or estimated from open site data. The development and validation of effective canopy radiation transfer models requires detailed sub-canopy radiation data measured at high temporal resolution (Flerchinger *et al*., 1996; Ni *et al*., 1997; Pearson *et al*., 1999; Hardy *et al*., 2004; Tribbeck *et al*., 2004). Detailed data are needed to validate radiative transfer models, because transmission of radiation through vegetation canopies is a function of angular and spectral distribution of the radiation (i.e. direct solar, diffuse solar, thermal), canopy species, height, density, structure, and albedo.

A variety of techniques are used to measure radiation beneath forest canopies. Early investigations used arrays of alcohol-distillation radiation integrators to obtain daily values of incoming solar radiation (Vézina,

* Correspondence to: Timothy E. Link, Department of Forest Resources, College of Natural Resources, PO Box 441133, Moscow, ID 83844-1133, USA. E-mail: tlink@uidaho.edu

Received 14 June 2004
Accepted 28 September 2004

1964). Strategically placed single radiometers have been used for woodland studies (Lafleur and Adams, 1986); however, single fixed radiometers are not appropriate for the rigorous characterization of the sub-canopy radiative regime due to the spatial variability resulting from canopy gaps. Pomeroy and Dion (1996) used tube radiometers designed for crop canopies, which integrate over a 100 cm length within high-latitude, dense, homogeneous canopies where sub-canopy radiation variability is relatively low. Tests indicated that these radiometers were adequate for measuring hourly averages of incoming and reflected shortwave radiation, and for studying canopy transmissivity when a large dataset (several months) from various solar paths was available, provided that the canopy was relatively dense and uniform. In environments where the spatial variability of radiation is higher, these sensors should be used with caution, since they integrate over a relatively small area. Automated tram-mounted radiometers that traverse 30–60 m transects have been used for warm-season investigations (e.g. Blanken *et al*., 2001; Law *et al*., 2001; Vrugt *et al*., 2002). During the winter months these systems are difficult to operate at the snow surface due to changing snowcover depth, snowfall and icing. The sampling area of these systems is also limited to the area traversed by the track, and information about the spatial radiative structure is difficult to obtain with these systems.

Arrays of pyranometers and pyrgeometers can be randomly deployed to integrate radiation at the snow surface and to measure the fine-scale spatial radiation structure beneath forest canopies. These systems are highly portable and can be installed directly on the snow surface beneath a variety of vegetation canopies. These sensor systems can be used to derive canopy characteristics when interrogated at high temporal resolutions. A variety of snowcover investigations with a range of canopy properties used data from radiometer arrays (Lafleur and Mantha, 1994; Hardy *et al*., 1997, 1998, 2004; Ni *et al*., 1997; Link and Marks, 1999b; Marks *et al*., 2001; Melloh *et al*., 2002; Rowlands *et al*., 2002; Sicart *et al*., 2004); however, the techniques and resulting data have not previously been described in detail.

The objective of this paper is to present a technique that can be used to quantify the transmissivity of a vegetation canopy to solar beam and diffuse radiation, and assess the thermal radiation emission from a canopy. Specifically, we present details of the sensors used, sensor installation, examples of resulting data, and a discussion of how canopy transmission parameters can be derived from sub-canopy radiation data.

METHODS

In this study, radiometer arrays used for sub-canopy investigations consisted of 9 to 20 pyranometers for the measurement of solar radiation and two or three pyrgeometers for the measurement of thermal radiation. Pyranometers used include Eppley precision spectral pyranometers (PSPs; 0·285–2·8 μm spectral range) and Kipp & Zonen CM-3 (0·305–2·8 μm spectral range) pyranometers. Thermopile-based sensors, which are sensitive to the full solar spectrum, are preferable for measurements within coniferous canopies. Silicon photodiode-based sensors (e.g. Li-Cor pyranometers) are only sensitive to wavelengths between approximately 0·4 and 1·1 μm, with a peak sensitivity around 0·9 μm. These sensors should, therefore, be used with caution in coniferous canopies where photosynthetically active radiation is depleted, but they are an inexpensive alternative for leafless deciduous canopies. Pyrgeometers used include Eppley precision infrared radiometers (PIRs; 3·5–50 μm spectral range) and Kipp & Zonen CG-1 (5–42 μm spectral range) sensors. All sensors were wired to an analogue multiplexer (Campbell Scientific Inc., AM416), which was attached to a datalogger (Campbell Scientific Inc., CR10X). Systems used for these investigations can be transported in two or three durable waterproof cases, one of which houses the datalogger base station and one or two which are used to transport the sensors. All sensors were calibrated on a regular basis, depending on manufacturer's specifications and the extent of their use.

Sensors were randomly distributed over a 25 m diameter circular area by selecting a random azimuth and distance from the datalogger system, such that some sensors were located within canopy gaps and some sensors were located next to tree stems. Radiometers were placed on wood or rigid styrofoam bases directly on the snow or ground surface. Sensors were levelled at least two times per day, usually around midday and at dusk, which allowed the bases to freeze into the snowpack overnight, stabilizing the sensor for the following day. Sensors were checked and cleaned of frost or dew at dawn, and were regularly cleaned during snowfall events. Sensors were interrogated every 10 s and averaged over 1 to 5 min intervals for final storage over a period of 3–5 days. Sensors were randomly relocated each day to increase further the number of sampling points within the canopy. An open-site reference array consisting of a pyranometer, pyrgeometer, datalogger and battery was used for studies where open-site radiation data were not part of the research site infrastructure. The reference array can be installed either above the canopy if an access tower is present, or at a nearby location unobstructed by terrain or vegetation. Diffuse solar radiation was also measured or estimated at each site.

Data are presented from three sites to illustrate how radiometer array data are used to quantify solar radiation transmission and thermal emission (Table I). These sites were selected because they represent a broad range of canopy transmissivities (33% to 3%), all had open-site or above-canopy solar and thermal radiation measurements, and two had diffuse radiation measurements with a shadow-band radiometer. The most transmissive (33%) of the three sites was a 17·5 m high leafless old aspen canopy (OA) located in the Southern Study Area (SSA) of the Boreal Ecosystem–Atmosphere Study (BOREAS) in central Saskatchewan, Canada (Chen *et al*., 1997a; Blanken *et al*., 2001). The SSA-OA site had a combined overstorey and understorey leafless wood area index WAI $\approx$ 1 (Chen *et al*., 1997a). The site with moderate transmissivity (15%) was a 12 m high old jack pine forest (SSA-OJP) having a leaf area index LAI = 2·5, also located in central Saskatchewan, Canada (Chen *et al*., 1997b). The least transmissive (3%) site was a 55–65 m high old-growth seasonal temperate rainforest, with LAI $\approx$ 8·6, located at the Wind River Canopy Crane Research Facility (WRCCRF) in Washington State, USA (Thomas and Winner, 2000). Detailed site information for the BOREAS project is provided by Sellers *et al*. (1997) and details of the WRCCRF are provided in Shaw *et al*. (2004).

RESULTS

Radiation measurements from the three canopies are shown in Figures 1–3. A summary of canopy solar radiation transmissivity and thermal radiation enhancement is presented in Table II. These transmissivity values depend on atmospheric conditions (e.g. solar zenith angle, air temperature, and humidity) and, therefore, are applicable to just the sampling periods noted. The advantage of collecting high-resolution data over several clear days is that the transmission characteristics of the canopy can be determined for a broad range of zenith angles.

Table I. Site characteristics

Site variable	Mature boreal aspen (leafless) with hazelnut understorey	Mature boreal jack pine	Old-growth temperate rainforest
Location	Saskatchewan, Canada	Saskatchewan, Canada	Washington State, USA
Latitude (°)	53·6289	53·9163	45·8205
Longitude (°)	−106·1978	−104·6920	−121·9519
Elevation (m a.m.s.l.)	601	579	370
Dominant species	Aspen/hazelnut	Jack pine	Douglas fir/western hemlock
LAI	0·62/0·34 (leafless wood area index)[a]	2·5[b]	8·6[c]
Canopy height (m)	21·5[b]	17[b]	55[d]
Stem density (ha^{-1})	828[b]	1600–4000	429[d]
Measurement period	4–8 March 1996	6–10 February 1994	22–24 September 2000

[a] Blanken *et al*. (2001).
[b] Chen *et al*. (1997a).
[c] Thomas and Winner (2000).
[d] Shaw *et al*. (2004).

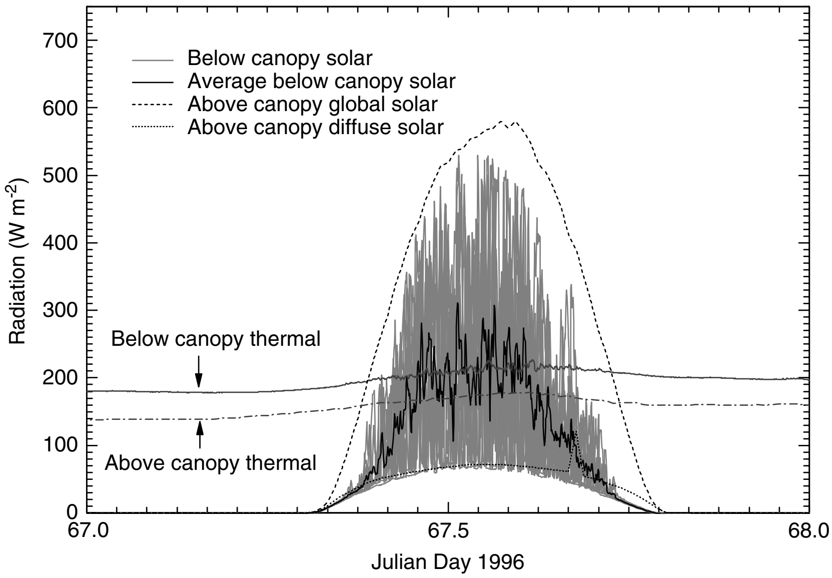

Figure 1. Radiation data collected above and below a mature boreal aspen canopy (SSA-OA)

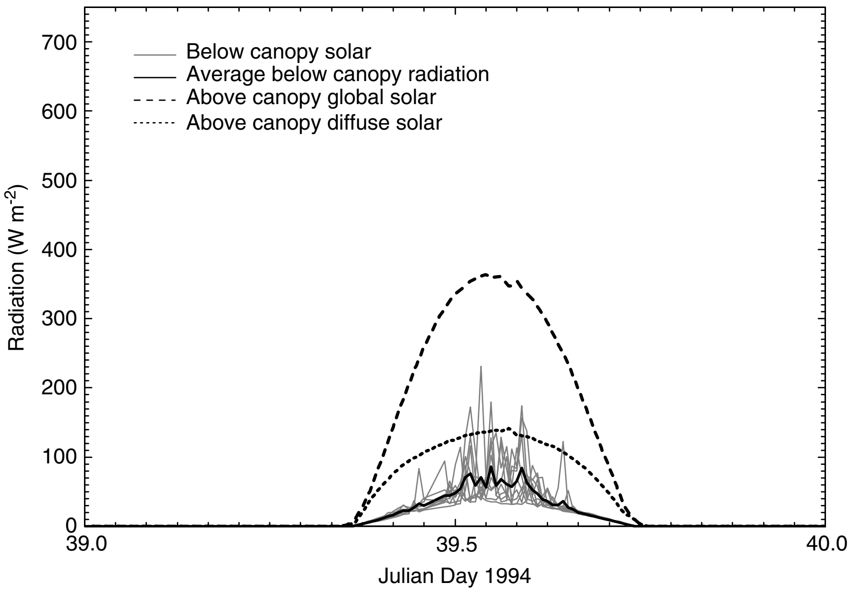

Figure 2. Radiation data collected above and below a mature boreal jack pine canopy

At the SSA-OA stand the data presented were collected over one almost completely clear day with a diffuse radiation spike in late afternoon probably associated with an isolated cloud (Hardy *et al.*, 1998) (Figure 1). Solar radiation below the canopy was highly variable, as shown by the data from the 10 individual radiometers (thin grey lines). The observed variability was due in part to the leafless deciduous canopy and to the 1 min averaging interval at this site. Individual sensors were at times completely shaded, producing an approximate average below-canopy diffuse radiation curve. The diffuse radiation measured above the canopy was approximately equal to the below-canopy diffuse radiation, due in part to the relatively high-albedo

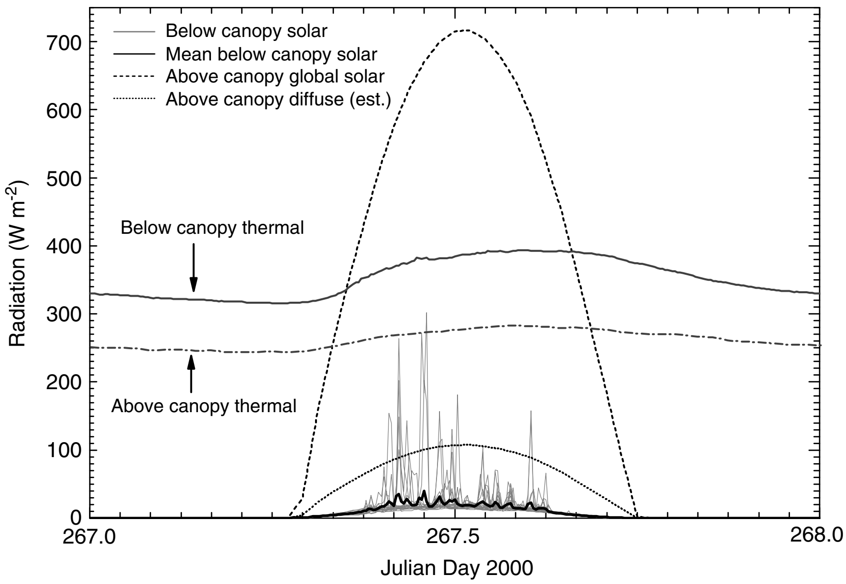

Figure 3. Radiation data collected above and below a seasonal temperate rainforest canopy

Table II. Summary of results

Variable	Mature boreal aspen (leafless)	Mature boreal jack pine	Old-growth temperate rainforest
Number of sensors	10	9	20
Maximum solar elevation angle (°)	31·0	19·1	43·0
Solar day-length (h)	10·5	8·5	12·0
Confidence coefficient for daily mean incoming solar radiation (95% CI)	6·6	7·8	7·2
Average solar transmissivity (%)	33·0	15·0	2·8
Average thermal enhancement (%)	24·8	nd	34·3
Net all-wave incoming radiation decrease (%)	21·6	nd	24·7
k_g (m^{-1})	0·019	0·033	0·038
τ_d (dimensionless)	0·44	0·20	0·08
k_b (m^{-1})	0·025	0·040	0·044

nd: no data.

smooth bark characteristic of aspens. In the early morning and evening periods, when solar elevation angles are low, almost all direct radiation was blocked by canopy elements; therefore, almost all radiation at the snow surface was diffuse. During these periods, the average of all sub-canopy sensors coincides with the sub-canopy diffuse radiation curve. Once the solar elevation is high enough for direct radiation to penetrate the canopy and produce sunflecks, the radiation received by individual sensors almost equals above-canopy radiation values. Direct radiation at the snow surface was observed for 6 h of the 10·5 h day. The average sub-canopy global radiation during the midday period still exhibits some variability, since the position of the 10 sensors did not completely average the spatial variability of the stand.

Despite the relative sparseness of the SSA-OA stand, the average transmissivity to solar radiation was only 33%, due to low winter sun angles in high-latitude regions (Table II). Computing a standard confidence coefficient (Ott, 1992), we found that true mean daily incoming solar radiation was within ±6·6% of the average array value at the 95% confidence level. The transmissivity contrasts with a 58% transmissivity value derived from radiation measurements prior to leaf-out on an automated tram mounted 4 m above the ground in the same canopy 2 years prior (Chen *et al*., 1997a). In their analysis of how the overstorey affected the radiation regime above the understorey, Chen *et al*. (1997a) noted that the solar zenith angle only has a small effect on solar radiation transmission, due to an increase in diffuse radiation that partially compensates for the decrease in beam radiation. The shape of the sub-canopy diffuse radiation trend obtained with the radiometer array is very similar to the above-canopy diffuse radiation trend, suggesting that diffuse radiation enhancement is unlikely at high zenith angles. The differences between these two methods are likely due to the sensor locations; the tram system was mounted at 4 m above the ground, whereas the radiometer array was placed directly on the snow surface, approximately 0·5 m above the ground, and beneath a 2 m high hazelnut understorey canopy. These data suggest that the understorey strongly affects the amount of solar radiation reaching the snow surface, and illustrates the importance of measuring radiation at the snow surface for snowcover investigations.

Above- and below-canopy measured thermal radiation is also shown in Figure 1. The total thermal radiative energy at the snow surface on this day was 24·8% higher than the total thermal radiative energy above the forest canopy due to emissivity differences between the canopy and sky, and due to heating of the canopy. On this day, the total all-wave radiative energy at the snow surface was 21·6% less than the above-canopy energy due to the combination of solar reduction and thermal enhancement.

Radiation data collected above and below a mature boreal jack pine (SSA-OJP) canopy in early February are shown in Figure 2 (Hardy *et al*., 1997). These data are for a clear day, as shown by the nearly perfect sinusoidal above-canopy radiation curve. Above-canopy diffuse radiation was relatively high during this period due to low sun angles (Table II) and long atmospheric path lengths characteristic of high latitudes in winter. Although the sensors were averaged over 5 min intervals, a sub-canopy diffuse radiation curve is also evident in these data. The old jack pine canopy also exhibited a similar, though less pronounced, increase in both the magnitude and variability of sub-canopy radiation around midday due to direct radiation penetration. Direct radiation penetration of the canopy was observed for 3·5 h of the 8·5 h day. At this site, the average transmissivity to solar radiation was 15%, due to a denser canopy and lower solar elevation angles relative to the old aspen site (Table II). The computed confidence coefficient shows that the true mean incoming below-canopy solar radiation is within $\pm 7{\cdot}8\%$ of the measured average at the 95% confidence interval. This slight increase in measurement variance may be because only nine radiometers were used, but it is most likely due to the lower transmissivity and the likelihood that the few sunflecks that do reach the snow surface will strike only a few radiometers. Thermal radiation data were not collected at this site.

Radiation data collected above and below a closed canopy area in an old-growth seasonal temperate rainforest (WRCCRF) stand in late September are shown in Figure 3. Even though these data were not collected in the winter, they are included as an example of a canopy with an extremely low transmissivity. These data are also from an exceptionally clear day, as shown by the perfect sinusoidal above-canopy radiation curve. In the absence of shadow-band radiometer data, above-canopy diffuse radiation was estimated assuming that this component comprised 15% of the above-canopy global radiation (a typical September value for this region). A very small proportion of above-canopy direct and diffuse radiation is transmitted through the canopy due to the low albedo and dense canopy, as shown by the average measured below-canopy radiation values. Furthermore, maximum values recorded by individual radiometers are much less than the above-canopy values. This is likely due to the brief temporal persistence of individual sunflecks coupled with the 5 min averaging interval. Average solar radiation transmissivity in this canopy was 2·8%, and direct radiation was only observed for approximately 6 h centred on solar noon. At lower sun angles in the morning and afternoon almost no solar radiation reaches the canopy floor. In this canopy, the computed confidence coefficient showed that true mean below-canopy solar radiation was within 7·2% of the measured average value at the 95% confidence interval, based on 20 sampling points (Table II).

The strong thermal radiation enhancement in this canopy is also evident in Figure 3. Below-canopy thermal radiation increases more rapidly than above-canopy thermal radiation in the morning hours due to canopy

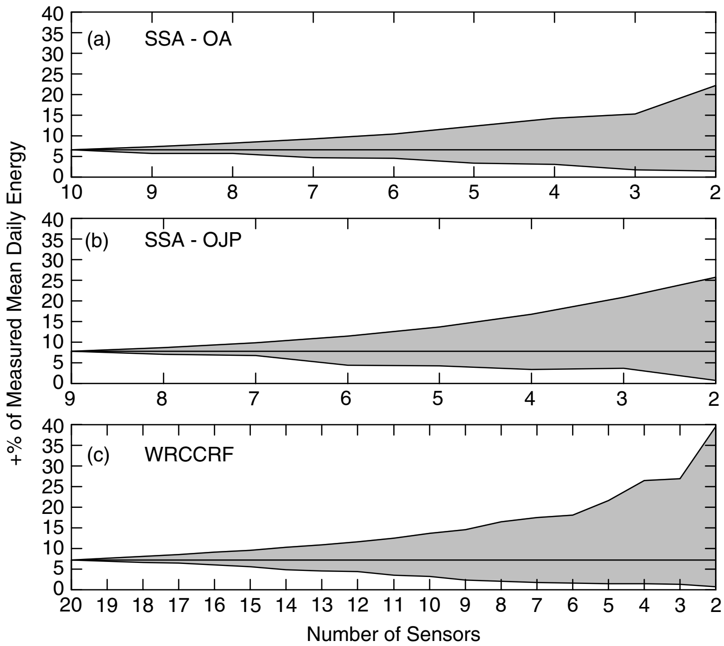

Figure 4. Maximum increases and decreases in the estimated accuracy of daily integrated radiation for simulated arrays with fewer sensors. Accuracy bounds were determined by selectively removing individual sensor records from each dataset in order to maximize the increase or decrease the sample variance

warming. During this period, average thermal radiation enhancement was 32%. The thermal enhancement partially offsets the solar reduction, resulting in a daily net all-wave incoming radiation decrease of 24·7% at the canopy floor.

As fewer sensors are used for sub-canopy radiation measurements, the estimated accuracy of the daily integrated measurement could either increase, if sensors were fortuitously located in areas with low radiation variance, or more likely would decrease due to the likelihood of having a larger sample variance. To assess the maximum increase or decrease in estimated accuracy resulting from use of fewer sensors, the confidence statistics were recomputed by selectively removing individual sensor records from each dataset to produce either the maximum decrease or increase in total sample variance. If the confidence statistics were recomputed with random sets of sensors, then the accuracy would fall within the grey-shaded fields in Figure 4. The potential accuracy of the daily integrated radiation decreased the least with a decrease in sensors at the SSA-OA site, due to the relatively homogeneous nature of the canopy (Figure 4a). The potential accuracy decreased the most in the old-growth conifer canopy due to a higher sample variance resulting from more heterogeneous canopy conditions and lower solar zenith angles (Figure 4c). This analysis indicates that a greater number of sensors are needed to compute accurate sub-canopy radiation in discontinuous canopies and at locations or during time periods with low zenith angles. It is difficult to determine *a priori* how many sensors will be needed to measure daily radiation with a specified degree of confidence in a given canopy. Sensors can be randomly relocated daily over successive days, effectively increasing the number of sampling locations in canopies where the variance in daily radiation is not known.

DISCUSSION

The three examples of sub-canopy radiation data presented indicate that arrays of around 10 radiometers can be used to produce reasonable estimates (i.e. computed confidence coefficients show that the true mean is within better than ±10% of the measured average) of average daily sub-canopy solar radiation. Measurement accuracy is improved by using more sensors, or randomly relocating sensors daily over a series of successive clear days, and averaging the data from the ensemble of sampling days. For example, at WRCCRF the computed confidence coefficient shows that the true mean daily incoming solar radiation was within 9·5% of the measured average at the 95% confidence level using data from the first 10 sensors, but only decreased to 7·2% when 20 sensors were used.

Mean sub-canopy solar radiation data can be used to compute the transmission coefficient for a given stand, defined simply as the ratio of below-canopy to above-canopy radiation. These data may also be used to compute the canopy extinction coefficient k for simple global radiative transfer estimation based on the Beer–Bouger–Lambert law

$$k = \frac{-\cos\theta}{h} \ln\left(\frac{S}{S_o}\right) \tag{1}$$

where θ is the zenith angle, h is the height of the canopy, S is the solar radiation below the canopy, and S_o is the unattenuated solar radiation (from Campbell and Norman (1998)).

Extinction coefficients for global radiation k_g were estimated by optimizing k in Equation (1) so that the computed S matched the mean below-canopy S integrated over a daily cycle (Table II). Extinction coefficients ranged from 0·019 m^{-1} in the aspen canopy to 0·038 m^{-1} in the rainforest canopy.

More accurate estimates of solar radiation at the snow surface may be obtained by treating the transmission of beam and diffuse radiation separately. This is desirable for snowcover studies, because the snowpack albedo for diffuse radiation is typically higher than for direct radiation (Male and Granger, 1981). Diffuse and direct albedo values may, therefore, be applied to the separate radiation streams to compute net snowcover radiation more accurately. Transmission of diffuse radiation may be estimated by computing a simple transmission coefficient τ_d:

$$\tau_d = \frac{S_d}{S_{d,o}} \tag{2}$$

where S_d is the diffuse radiation at the snow surface and $S_{d,o}$ is the diffuse radiation at an unobstructed location. The extinction coefficient for direct beam radiation k_b can be estimated using Equation (1) as described above, where S and S_o are direct radiation values.

An example of how radiometer array data may be used to derive canopy parameters for more rigorous methods that treat the transmission of direct and diffuse radiation separately is shown in Figure 5 (e.g. Link and Marks, 1999b). Measured above-canopy global and diffuse solar radiation and below-canopy global radiation are shown in Figure 5a. An estimate for τ_d may be obtained from these data, since the relatively high temporal sampling interval (i.e. 1 to 5 min) produces a distinct sub-canopy diffuse solar radiation trend. Above-canopy diffuse radiation was multiplied by τ_d, until the resulting curve matched the approximate sub-canopy diffuse radiation curve (Figure 5b). The sub-canopy direct radiation was estimated by subtracting the estimated sub-canopy diffuse values from the average measured sub-canopy global values from the array (Figure 5c). The extinction coefficient for direct radiation k_b was then derived by optimizing k_b so that the computed sub-canopy direct radiation matched the measured daily total. The resulting canopy parameters (Table II) were used to estimate the below-canopy solar radiation from a combined version of Equations (1) and (2):

$$S_g = \tau_d S_{d,o} + S_{b,o}\, e^{-hk_b/\cos\theta} \tag{3}$$

where subscripts '*g*', '*d*', and '*b*' refer to global, diffuse, and direct radiation respectively, and '*o*' refers to unobstructed locations. The average measured below-canopy global radiation and resulting estimated values are shown in Figure 5d. The advantage of using separate transmission and extinction coefficients for beam and diffuse radiation is that the shape of the within-canopy radiation curve is more accurately reproduced relative to using a single extinction coefficient for global radiation (e.g. Campbell and Norman, 1998).

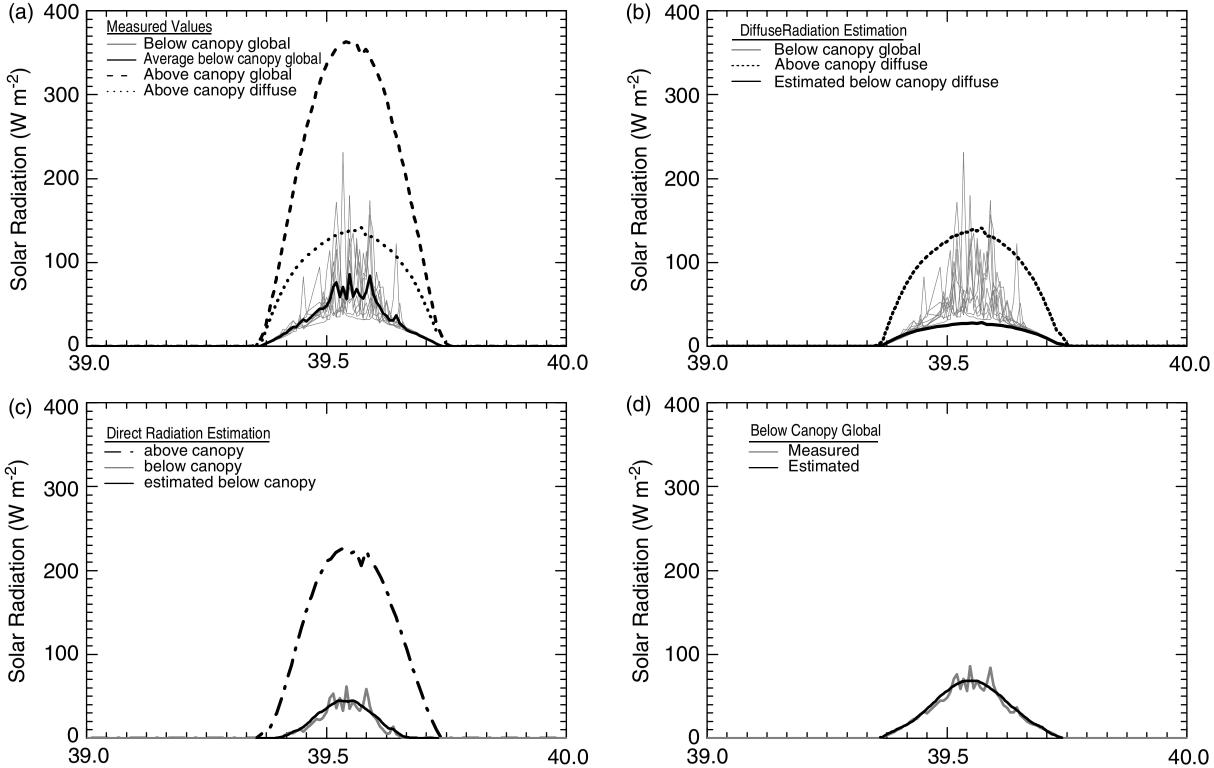

Figure 5. Example from the SSA-OJP site of how canopy parameters may be derived from radiometer array data. (a) Measured open and below solar radiation data. (b) The diffuse transmission factor τ_d is estimated from Equation (2) by visually matching the estimated curve to the curve determined from the array data. (c) Direct radiation below the canopy is estimated by subtracting the estimated below-canopy diffuse radiation from the mean below-canopy global radiation. The extinction coefficient for direct radiation (k_b) is determined by optimizing Equation (1) for total solar energy received over the interval. (d) Below-canopy global radiation is estimated from Equation (3)

The technique described above is complicated by multiple scattering within canopies, thereby causing a portion of beam radiation above the canopy to be transformed into diffuse radiation at the snow surface. Data from radiometer arrays may also be used to assess within-canopy scattering when collected over a combination of completely cloudy and clear days. For example, τ_d is best derived on a day when the above-canopy radiation is completely diffuse and, therefore, all sub-canopy radiation is diffuse. The difference between the computed sub-canopy diffuse radiation and the measured sub-canopy diffuse radiation on a clear day can be used to estimate the proportion of direct radiation that is scattered in a given canopy. Canopy parameters computed for the jack pine and aspen/hazelnut canopies indicated that the jack pine scattered a negligible portion of the direct radiation, whereas the aspen/hazelnut canopy scattered ~7% of the direct radiation. These results are reasonable given the low albedo and rough bark of the conifer canopy compared with the relatively smooth bark and reflective characteristics of the overstorey aspen canopy. Ideally, radiation measurements should be made during both cloudy and clear conditions to reduce errors in the determination of the transmission coefficients.

Radiative transfer models using canopy parameters derived from radiometer array measurements have been used to simulate sub-canopy snowcover dynamics effectively (Hardy *et al*., 1997, 1998, 2004; Link and Marks, 1999a,b; Marks *et al*., 2001; Melloh *et al*., 2002). Simulated snowcover dynamics were relatively insensitive to canopy transmissivity parameters, since errors in solar transmission were partly balanced by counteracting errors in thermal emission (Link and Marks, 1999b). This observation suggests that, where general canopy characteristics are known, transmissivity and emissivity parameters may be estimated from similar sites where array data have been collected. For example, accurate snowmelt simulations were achieved in mid-latitude aspen and fir stands, using canopy parameters derived from boreal aspen and jack pine stands with similar structural characteristics (Marks *et al*., 2001).

Radiometer arrays are also useful for focused investigations of radiative transfer as related to canopy structure when deployed in non-random patterns. For example, radiometers placed in a radial pattern away from individual tree stems were used to assess the fine-scale variability of radiation with tree wells (Hardy *et al*., 2002). Sensors may similarly be configured as a linear array to assess the variation in radiative transfer across forest-open, or other canopy discontinuities.

One potential limitation of radiometer array-based measurements of sub-canopy radiation for snowmelt investigations is that standard thermopile-based pyranometers measure total solar radiation over wavelengths from ~0·3 to 3·0 μm. Coniferous canopies preferentially absorb visible (0·3–0·7 μm) wavelengths but are reflective in the near-infrared (NIR, 0·7–3·0 μm). Snow, however, is highly reflective in the visible portion of the spectrum, and more absorptive in the NIR, especially during melt, when the snow surface is wet (Warren, 1982). Studies in mixed canopies indicated that this spectral shift coupled with deposition of organic debris lowers the snow albedo in forested areas relative to open areas (Melloh *et al*., 2002). Additional spectral information in other coniferous forests may, therefore, improve our understanding of snowmelt dynamics beneath forest canopies.

In the examples presented here, thermal radiation was measured with two to four sensors. Thermal radiation is completely diffuse, with very little observed variation (i.e. <25 W m^{-2}) observed between sensors placed beneath relatively dense tree crowns and small gaps between trees. In more open canopies, and during times of the year where zenith angles are lower, we expect that thermal radiation would exhibit greater spatial and temporal variability due to a wider variability in the hemispheric sky view factor under the canopy and heating of canopy elements by direct solar radiation. Additional research is needed to assess both the solar and thermal radiation regime in sparse and discontinuous canopies.

SUMMARY AND CONCLUSIONS

Solar and thermal radiometer arrays are robust, highly portable tools that can be easily deployed at the snow surface beneath a wide variety of vegetation canopies. Radiometer arrays provide measurements of spatially averaged direct and diffuse radiation within forest canopies when sampled at a high temporal resolution. These data have been used for a variety of applications, including inputs to snowmelt models and for development, validation, and parameterization of canopy radiative transfer models. Although more-complex canopy radiative transfer models exist, simple, computationally efficient algorithms parameterized with radiometer array data are advantageous for spatially distributed snowcover simulations. Data from array-based measurements can also be used to address other questions, such as how canopy transmissivity changes seasonally, or how transmissivities change spatially within open canopies or across land-cover discontinuities. Radiometer arrays may also be used other for hydrologic or water quality investigations, including evaporation dynamics beneath forest canopies, or assessing how streamside vegetation affects the radiative regime of stream systems.

ACKNOWLEDGEMENTS

We wish to thank Dr John Pomeroy and two anonymous reviewers whose comments improved this paper. Support for this research was provided by NASA (grant NAG5-2301, reference 2207-BOREAS-U107, and grant POS-12856-F, reference 2250-BOREAS-U150), by the Office of Science, Biological and Environmental Research Program (BER), US Department of Energy, through the Western Regional Center (WESTGEC) of the National Institute for Global Environmental Change (NIGEC) under Cooperative Agreement No. DE-FC03-90ER61010, and supplemented by US Army Project 4A762784AT42. Additional support was provided by the USDA-ARS Northwest Watershed Research Center. We thank the Saskatchewan Research Council and Wind River Canopy Crane Research Facility for meteorological data, as well as Bert Davis and Bryan Harrington of ERDC-CRREL.

Mention of product brand names and specific instruments is for clarity and is not intended as a recommendation or endorsement of specific products.

REFERENCES

Blanken PD, Black TA, Neumann HH, den Hartog G, Yang PC, Nesic Z, Lee X. 2001. The seasonal water and energy exchange above and within a boreal aspen forest. *Journal of Hydrology* **245**: 118–136.

Campbell GS, Norman JM. 1998. *An Introduction to Environmental Biophysics*. Springer-Verlag: New York.

Chen JM, Blanken PD, Black TA, Guilbeault M, Chen S. 1997a. Radiation regime and canopy architecture in a boreal aspen forest. *Agricultural and Forest Meteorology* **86**: 107–125.

Chen JM, Rich PM, Gower ST, Norman JM, Plummer S. 1997b. Leaf area index of boreal forests: theory, techniques, and measurements. *Journal of Geophysical Research–Atmospheres* **102**: 29 429–29 443.

Flerchinger GN, Baker JM, Spaans EJA. 1996. A test of the radiative energy balance of the SHAW model for snowcover. *Hydrological Processes* **10**: 1359–1367.

Hardy JP, Davis RE, Jordan R, Li X, Woodcock C, Ni W, McKenzie JC. 1997. Snow ablation modeling at the stand scale in a boreal jack pine forest. *Journal of Geophysical Research* **102**: 29 397–29 405.

Hardy JP, Davis R, Jordan R, Ni W, Woodcock CE. 1998. Snow ablation modelling in a mature aspen stand of the boreal forest. *Hydrological Processes* **12**: 1763–1778.

Hardy J, Pomeroy J, Rowlands A, Marks D, Melloh R, Koenig G. 2002. Solar and longwave radiation dynamics around a single conifer tree with implications for snow modeling in forests. *Eos, Transactions, American Geophysical Union* **83**: F537.

Hardy JP, Melloh R, Marks D, Koenig G, Winstral A, Pomeroy JW, Link TE. 2004. Solar radiation transmission through conifer canopies. *Agricultural and Forest Meteorology* **126**: 257–270.

Lafleur PM, Adams P. 1986. The effect of subarctic woodland vegetation on the radiation balance of a melting snow cover. *Archives for Meteorology, Geophysics and Bioclimatology* **34**: 297–310.

Lafleur PM, Mantha BK. 1994. Global radiation within subarctic open forest canopies. *Canadian Journal of Forest Research* **24**: 1062–1066.

Law BE, Van Tuyl S, Cescatti A, Baldocchi DD. 2001. Estimation of leaf area index in open-canopy ponderosa pine forests at different successional stages and management regimes in Oregon. *Agricultural and Forest Meteorology* **108**: 1–14.

Link TE, Marks D. 1999a. Distributed simulation of snowcover mass- and energy-balance in the boreal forest. *Hydrological Processes* **13**: 2439–2452.

Link TE, Marks D. 1999b. Point simulation of seasonal snow cover dynamics beneath boreal forest canopies. *Journal of Geophysical Research* **104**: 27 841–27 857.

Male DH, Granger RJ. 1981. Snow surface energy exchange. *Water Resources Research* **17**: 609–627.

Marks D, Link T, Winstral A, Garen D. 2001. Simulating snowmelt processes during rain-on-snow over a semi-arid mountain basin. *Annals of Glaciology* **32**: 195–202.

Melloh R, Hardy JP, Bailey R, Hall T. 2002. An efficient snow albedo model for the open and sub-canopy. *Hydrological Processes* **16**: 3571–3584.

Ni W, Li X, Woodcock CE, Roujean JL, Davis RE. 1997. Transmission of solar radiation in boreal conifer forests: measurement and models. *Journal of Geophysical Research* **102**: 29 555–29 556.

Ott RL. 1992. *An Introduction to Statistical Methods and Data Analysis*, 4th edition. Duxbury Press: Belmont, CA.

Pearson D, Daamen CC, Gurney RJ, Simmonds LP. 1999. Combined modelling of shortwave and thermal radiation for one-dimensional SVATs. *Hydrology and Earth Systems Science* **3**: 15–30.

Pomeroy JW, Dion K. 1996. Winter radiation extinction and reflection in a boreal pine canopy: measurements and modelling. *Hydrological Processes* **10**: 1591–1608.

Rowlands A, Pomeroy J, Hardy J, Marks D, Elder K, Melloh R. 2002. Small-scale variability of radiant energy for snowmelt in a mid-latitude sub-alpine forest. In *Eastern Snow Conference*; 93–108.

Sellers PJ, Hall FG, Kelly RD, Black A, Baldocchi D, Berry J, Ryan M, Ranson KJ, Crill PM, Lettenmaier DP, Margolis H, Cihlar J, Newcomer J, Fitzjarrald D, Jarvis PG, Gower ST, Halliwell D, Williams D, Goodison B, Wickland DE, Guertin FE. 1997. BOREAS in 1997: experiment overview, scientific results, and future directions, *Journal of Geophysical Research* **102**: 28 731–28 769.

Shaw DC, Franklin JF, Bible K, Klopatek J, Freeman E, Greene S, Parker GG. 2004. Ecological setting of the Wind River old-growth forest. *Ecosystems* **7**: 427–439. DOI: 10.1007/s10021-004-0135-6.

Sicart J, Pomeroy J, Essery R, Hardy J, Link T, Marks D. 2004. A sensitivity study of daytime net radiation during snowmelt to forest canopy and atmospheric conditions. *Journal of Hydrometeorology* **5**: 774–784.

Thomas SC, Winner WE. 2000. Leaf area index of an old-growth Douglas-fir forest estimated from direct structural measurements in the canopy. *Canadian Journal of Forest Research* **30**: 1922–1930.

Tribbeck MJ, Gurney RJ, Morris EM, Pearson D. 2004. A new snow-SVAT to simulate the accumulation and ablation of seasonal snowcover beneath a forest canopy. *Journal of Glaciology* in press.

Vézina PE. 1964. Solar radiation available over snow pack in a dense pine forest. *Agricultural and Forest Meteorology* **1**: 54–65.

Vrugt JA, Bouten W, Dekker SC, Musters PAD. 2002. Transpiration dynamics of an Austrian pine stand and its forest floor: identifying controlling conditions using artificial neural networks. *Advances in Water Resources* **25**: 293–303.

Warren SG. 1982. Optical properties of snow. *Reviews of Geophysics and Space Physics* **20**: 67–89.

